

1 **Variability of flow discharge in lateral inflow-dominated stream**
2 **channels**

3

4 Ching-Min Chang and Hund-Der Yeh*

5 Institute of Environmental Engineering,

6 National Chiao Tung University, Hsinchu, Taiwan

7

8 **Abstract.** The influence of the temporal changes in lateral inflow rate on the discharge
9 variability in stream channels is explored through the analysis of the diffusion wave
10 equation (i.e., the linearized Saint-Venant equation). To account for variability and
11 uncertainty, the lateral inflow rate is regarded as a temporal random function. On the
12 basis of the spectral representation theory, analytical expressions for the covariance
13 function and evolutionary power spectral density of the random discharge perturbation
14 process are derived to quantify variability in stream flow discharge induced by the
15 temporal changes in lateral inflow rate. The treatment of the discharge variance (square
16 root of the variance) gives us a quantitative estimate of uncertainty in predictions from
17 the deterministic model. It is found that the discharge variability of stream flow is very
18 large in the downstream reach, indicating large uncertainty anticipated from the use of the
19 deterministic model. A larger temporal correlation scale of inflow rate fluctuations,
20 representing more temporal consistency of fluctuations in inflow rate around the mean,
21 introduces a higher variability in stream flow discharge.

22

23 **1. Introduction**

24

25 Surface runoff originates from precipitation intensities exceeding the infiltration capacity
26 of the surface (e.g., Duan et al., 1992; Sivakumar et al., 2000; Ruiz-Villanueva et al.,
27 2012; Valipour, 2015). This process may result in lateral inflow to nearby stream channels.
28 Significant lateral inflows may contribute to streams during storm-runoff periods when
29 stream reaches are of large lateral watershed areas or upslope accumulated areas (Jencso
30 et al., 2009). These lateral inflows may be not only a source of water to streams, but also
31 a source of contaminants to surface water. Agricultural chemicals are frequently mixed
32 into shallow soil layers and lateral inflows may cause the release and migration of them
33 into streams (Govindaraju, 1996). The effect of the lateral inflow on the stream flow
34 provides an important basis for analyzing contaminant transport in surface water.
35 Understanding and quantification of the influence of inflow process on stream flow
36 discharge is therefore essential for water resource planning and management.

37 Natural variability, such as significant variability of rainfall events on both
38 temporal and spatial scales (e.g., Ogden and Julien, 1993; Redano and Lorente, 1993;
39 Wheater et al., 2000; Zhang et al., 2001; De Michele and Bernardara, 2005; Haberlandt et
40 al., 2008; Valipour, 2012; Bewket and Lal, 2014) and the great heterogeneity of soil types
41 at the ground surface (e.g., Jencso et al., 2009; Fournier et al., 2013) and surface
42 saturation (e.g., Schumann et al., 2009; Riley and Shen, 2014) over a watershed, creates a
43 very complex runoff process on the land surface. Many practical problems of flood wave
44 routing require predictions over relatively large time and space scales. The key issue is
45 how one can realistically incorporate the effect of natural heterogeneity into models to
46 predict flood wave behavior at large time and space scales. Due to a high degree of the

47 natural heterogeneity of the surface runoff process, the use of deterministic analysis
48 techniques in stream flow modeling is inevitably subject to large uncertainty. The
49 theoretical understanding of variability in flood wave routing is far from complete.
50 Motivated by that, this article focuses on quantification of the discharge variability in a
51 lateral-inflow-dominated stream.

52 In the follows, the response of transient stream flow process to spatiotemporal
53 lateral inflow in a diffusion wave model is analyzed stochastically by treating the
54 fluctuations in lateral inflow rate as temporal stationary random processes. The
55 non-stationary spectral techniques are employed to obtain closed-form solutions for
56 quantifying the discharge variability in stream channels. These solutions provide variance
57 relations for flow discharge, and thereby allow for assessing the impact of statistical
58 properties of lateral inflow rate process on the discharge variability.

59 To the best of our knowledge, the issue on quantifying the effect of temporal
60 variation of lateral inflow on the stream flow variability using non-stationary spectral
61 techniques so far has not been addressed. The approach presented herein provides not
62 only an analytical methodology but also a basic framework for understanding the
63 response of transient stream flow process and quantifying the stream flow variability. It
64 is hoped that the proposed approach and our findings obtained in this study are useful for
65 further research in this area.

66

67 **2. Description of the problem**

68

69 This study considers the case of unsteady flow in open channels. The equations that

70 describe the propagation of a flood wave with respect to distance along the channel and
 71 time in open channels, are the so-called Saint-Venant equations, consisting of the
 72 continuity equation and the momentum equation. For most flood events, in most rivers
 73 the inertial terms appearing in the momentum equation of the Saint-Venant equations can
 74 be neglected as they are relatively smaller than the terms arising from gravity and
 75 resistance forces (Henderson, 1963; Dooge and Harley, 1967; Daluz Viera, 1983),
 76 leading to a simplified model of open channel flow. The diffusion wave equation is then
 77 expressed as (e.g., Moussa, 1996; Sivapalan et al., 1997):

$$78 \quad \frac{\partial Q}{\partial t} + C_d(Q, \frac{\partial Q}{\partial X}) \left[\frac{\partial Q}{\partial X} - q_L \right] = \frac{1}{\sqrt{S_0}} \frac{\partial}{\partial X} \left[D_h(Q) \left(\frac{\partial Q}{\partial X} - q_L \right) \right]. \quad (1)$$

79 where Q is the discharge, C_d and D_h are non-linear function of discharge generally known
 80 as wave celerity and hydraulic diffusivity, respectively, S_0 is the bed slope, and $q_L(X, t)$
 81 represents the net lateral inflow distribution. The diffusion wave equation (1) is
 82 formulated by combining the continuity equations for both mass and momentum. The
 83 diffusion wave approximation is appropriate for simulations of the flood waves in rivers
 84 and on flood plains with milder slopes ranging between 0.001 and 0.0001
 85 (Kazezyılmaz-Alhan, 2012). Most natural flood waves can then be described with the
 86 diffusion wave model. Some of the successful applications of the simplified channel flow
 87 models to flood routing are available in the literature (e.g., Ponce et al., 1978; Singh and
 88 Aravamuthan, 1995; Moramarco and Singh, 2002; Khasraghi et al., 2015).

89 Equation (1) is a nonlinear partial differential equation and has a complex behavior
 90 of the stream flow in general. No analytical solution of Eq. (1) is available in the
 91 literature. However, the problem can be solved analytically by some simplifications to Eq.

92 (1), such as linearization for the case of an initially steady uniform flow. On the basis of
 93 expansion of the dependent variable and the nonlinear terms in Eq. (1) around the initial
 94 condition of steady uniform flow and limitation of the expansion to the first-order
 95 variation from the steady state, the resulting linearized Eq. (1) can be written as

$$96 \quad \frac{\partial Q'}{\partial t} = D \frac{\partial^2 Q'}{\partial X^2} - C \frac{\partial Q'}{\partial X} + [C q_L - D \frac{\partial q_L}{\partial X}] \quad (2)$$

97 In Eq. (2), $Q' = Q - Q_0$ ($Q_0 \gg Q', q_L$), Q_0 is the initial uniform steady-state flow discharge,
 98 and C and D represent constant celerity and diffusivity, respectively, depending on the
 99 initially uniform flow (velocity and flow depth). The reader may be referred to Dooge
 100 and Napiorkowski (1987), Ponce (1990), Yen and Tsai (2001) or Tsai and Yen (2001) for
 101 the detailed development.

102 The problem of interest here is the stream flow response to the temporal changes in
 103 lateral inflow rate, which is governed by Eq. (2). The solution to Eq. (2) with associated initial
 104 and boundary conditions will serve as the starting point for conducting the following
 105 investigation of stream flow variability.

106 To derive the analytical solution of Eq. (2), one needs to specify the form of $q_L(X, t)$.
 107 In the present work, the focus is placed on the case that the net lateral inflow is
 108 well-approximated by the following spatiotemporal distribution (e.g., Lane, 1982;
 109 Capsoni et al., 1987; Goodrich et al., 1997; Féral et al., 2003).

$$110 \quad q_L(X, t) = q_M(t) \exp\left(-\frac{X}{\eta}\right) \quad (3)$$

111 where q_M is the peak inflow rate, and η is the distance along the X -axis for which the
 112 inflow rate decreases by a factor e^{-1} with respect to q_M . In particular, q_M is considered to

113 be a temporally correlated stationary random field. It is apparent from Eq. (2) that the last
114 two terms associated with the lateral inflow are introduced as the sources of fluctuations
115 in stream flow discharge and treated here as temporally correlated stochastic processes.
116 Equation (2) is then viewed as a stochastic differential equation with a stochastic output
117 Q' . The solution of Eq. (2) will provide a rational basis for quantifying the flow
118 variability through the representation theorem.

119 Consider that the flow domain is bounded within the range $0 \leq X \leq L$. The associated
120 initial and boundary conditions can be expressed as

$$121 \quad Q'(X,0) = 0 \quad (4a)$$

$$122 \quad Q'(0,t) = 0 \quad (4b)$$

$$123 \quad \frac{\partial}{\partial X} Q'(L,t) = 0 \quad (4c)$$

124 Equations (4a) signifies that there is no perturbation from the reference discharge initially
125 while Eq. (4b) assumes no inflow at the upstream boundary at all times. The downstream
126 boundary condition represented by Eq. (4c) is under the condition of a zero-discharge
127 gradient. Morris (1979) showed that this downstream boundary condition is applicable to
128 a large class of problems.

129

130 **3. General solutions via spectral theory**

131

132 The approach followed is to develop the analytical solution of Eq. (2) in the Fourier
133 frequency domain.

134 Temporal stationarity of the q_M perturbation process admits a spectral representation

135 of the form (e.g., Priestley, 1965)

$$136 \quad q_L = q_M(t) \exp\left(-\frac{X}{\eta}\right) = \exp\left(-\frac{X}{\eta}\right) \int_{-\infty}^{\infty} e^{i\omega t} dZ_q(\omega) \quad (5)$$

137 where ω is the frequency parameter, $Z_q(\omega)$ is an orthogonal process, and dZ_q is a
138 zero-mean orthogonal increment process with

$$139 \quad E[dZ_q(\omega_1) dZ_q^*(\omega_2)] = S_{qq}(\omega_1) \delta(\omega_1 - \omega_2) d\omega_1 d\omega_2 \quad (6)$$

140 in which $E[-]$ denotes the ensemble average, the superscript asterisk stands for the
141 complex-conjugation operator, and $S_{qq}(-)$ is the power spectral density for the stationary
142 random q_M perturbation process. On the other hand, without the restriction on the
143 assumption of stationarity the random perturbed quantities Q' may be expressed in the
144 form of the Fourier-Stieltjes integral representation as (e.g., Priestley, 1965; Li and
145 McLaughlin, 1991)

$$146 \quad Q'(X, t) = \int_{-\infty}^{\infty} \Theta_{Qq}(X, t, \omega) dZ_q(\omega) \quad (7)$$

147 where $\Theta_{Qq}(-)$ is the transfer function depending on space, time, and frequency.

148 It follows from Eqs. (5) and (7) that Eq. (2) takes the form

$$149 \quad \frac{\partial \Theta_{Qq}}{\partial t} = D \frac{\partial^2 \Theta_{Qq}}{\partial X^2} - C \frac{\partial \Theta_{Qq}}{\partial X} + \exp\left(-\frac{X}{\eta} + i\omega t\right) \left(C + \frac{D}{\eta}\right) \quad (8)$$

150 subject to the following initial and boundary conditions

$$151 \quad \Theta_{Qq}(X, 0) = 0 \quad (9a)$$

$$152 \quad \Theta_{Qq}(0, t) = 0 \quad (9b)$$

$$153 \quad \frac{\partial \Theta_{Qq}}{\partial X}(L, t) = 0 \quad (9c)$$

154 The method of eigenfunction expansion is used to solve this inhomogeneous boundary
155 value problem, and the solution of Eq. (8) with Eq. (9) is:

$$156 \quad \Theta_{Qq}(X, t, \omega) = 2 \frac{D}{L} \left(\nu + \frac{1}{\mu} \right) \exp\left(\frac{\nu}{2} \xi\right) \sum_{n=0}^{\infty} \frac{a_n - \beta \exp(-\beta) \cos(n\pi)}{\beta^2 + a_n^2} \sin(a_n \xi) \\ 157 \quad \times \frac{\exp(-i\omega t) - \exp(-F_n t)}{F_n - i\omega} \quad (10)$$

158 where $\nu = CL/D$, $\mu = \eta/L$, $a_n = \pi(2n+1)/2$, $\xi = X/L$, $\beta = (\nu/2) + 1/\mu$, and $F_n = D[a_n^2 + \nu^2/4]/L^2$.
159 Rewriting Eq. (7), and using Eq. (10), yields the solution of Eq. (2) in the frequency
160 domain as

$$161 \quad Q'(X, t) = 2 \frac{D}{L} \left(\nu + \frac{1}{\mu} \right) \exp\left(\frac{\nu}{2} \xi\right) \sum_{n=0}^{\infty} \frac{a_n - \beta \exp(-\beta) \cos(n\pi)}{\beta^2 + a_n^2} \sin(a_n \xi) \\ 162 \quad \times \int_{-\infty}^{\infty} \frac{\exp(-i\omega t) - \exp(-F_n t)}{F_n - i\omega} dZ_q(\omega) \quad (11)$$

163 The covariance function of the flow discharge field, $C_{Qq}(-)$, can be computed on the
164 basis of the representation theorem for Q' by

$$165 \quad C_{Qq}(X, t_1, t_2) = E[Q'(X, t_1) Q'^*(X, t_2)] = \int_{-\infty}^{\infty} \Theta_{Qq}(X, t_1, \omega) \Theta_{Qq}^*(X, t_2, \omega) S_{qq}(\omega) d\omega \\ 166 \quad = 4 \frac{D^2}{L^2} \left(\nu + \frac{1}{\mu} \right)^2 \exp(\nu \xi) \sum_{m=0}^{\infty} \sum_{n=0}^{\infty} \frac{\sin(a_m \xi) \sin(a_n \xi)}{(\beta^2 + a_m^2)(\beta^2 + a_n^2)} \\ 167 \quad \times \{ a_m a_n - \beta \exp(-\beta) [a_m (-1)^m + a_n (-1)^n] + \beta^2 (-1)^{m+n} \exp(-2\beta) \}$$

168 $\times \int_{-\infty}^{\infty} \frac{\exp[i\omega(t_1 - t_2)] - \exp(-F_m t_1 - i\omega t_2) - \exp(i\omega t_1 - F_n t_2) + \exp(F_m t_1 + F_n t_2)}{(F_m F_n + \omega^2) + i \frac{D}{L^2} (a_n^2 - a_m^2) \omega} S_{qq}(\omega) d\omega$

169 (12)

170 where $a_m = \pi(2m+1)/2$ and $F_m = D[a_m^2 + \nu^2/4]/L^2$. The variance of flow discharge
 171 fluctuations is obtained by evaluating Eq. (12) at zero time lag as

172 $\sigma_Q^2(X, t) = C_{QQ}(X, t, t) = 4 \frac{D^2}{L^2} \left(\nu + \frac{1}{\mu}\right)^2 \exp(\nu \xi) \sum_{m=0}^{\infty} \sum_{n=0}^{\infty} \frac{\sin(a_m \xi) \sin(a_n \xi)}{(\beta^2 + a_m^2)(\beta^2 + a_n^2)}$

173 $\times \left\{ a_m a_n - \beta \exp(-\beta) [a_m (-1)^m + a_n (-1)^n] + \beta^2 (-1)^{m+n} \exp(-2\beta) \right\}$

174 $\times \int_{-\infty}^{\infty} \frac{1 - \exp[-(F_m + i\omega)t] - \exp[(i\omega - F_n)t] + \exp[(F_m + F_n)t]}{(F_m F_n + \omega^2) + i \frac{D}{L^2} (a_n^2 - a_m^2) \omega} S_{qq}(\omega) d\omega$ (13)

175 In addition, following Priestley (1965), the variance of the Q' process may be
 176 written in the form of

177 $\sigma_Q^2(X, t) = \int_{-\infty}^{\infty} |A_t(X, t, \omega)|^2 E[dZ_q(\omega) dZ_q^*(\omega)]$ (14)

178 so that the evolutionary power spectral density of the non-stationary random process can
 179 be defined as

180 $E[dZ_Q(X, t, \omega) dZ_Q^*(X, t, \omega)] = |A_t(X, t, \omega)|^2 E[dZ_q(\omega) dZ_q^*(\omega)]$ (15)

181 where $A_t(-)$ is referred to as the modulating function of the non-stationary process. The
 182 evolutionary spectrum has the same physical interpretation as the spectrum of a stationary
 183 process, namely, that it describes the distribution of mean square signal content (or
 184 fluctuations) of the random process at a given time t . Comparing Eq. (14) to Eq. (13)

185 leads Eq. (15) to

$$\begin{aligned}
186 \quad S_{\varrho\varrho}(X, t, \omega) &= 4 \frac{D^2}{L^2} \left(\nu + \frac{1}{\mu}\right)^2 \exp(\nu\xi) \sum_{m=0}^{\infty} \sum_{n=0}^{\infty} \frac{\sin(a_m \xi) \sin(a_n \xi)}{(\beta^2 + a_m^2)(\beta^2 + a_n^2)} \\
187 \quad &\times \left\{ a_m a_n - \beta \exp(-\beta) [a_m (-1)^m + a_n (-1)^n] + \beta^2 (-1)^{m+n} \exp(-2\beta) \right\} \\
188 \quad &\times \frac{1 - \exp[-(F_m + i\omega)t] - \exp[(i\omega - F_n)t] + \exp[(F_m + F_n)t]}{(F_m F_n + \omega^2) + i \frac{D}{L^2} (a_n^2 - a_m^2) \omega} S_{qq}(\omega) \quad (16)
\end{aligned}$$

189 where $S_{\varrho\varrho}(-)$ is the spectral density of the Q' perturbation process.

190 The infinite series in Eq. (10) converges rapidly when $\tau_c = Dt/L^2 \gg 1/\pi^2$.

191 Accordingly, Eq. (10) can reduce to

$$192 \quad \Theta_{\varrho q}(X, t, \omega) = \frac{D}{L} \left(\nu + \frac{1}{\mu}\right) \frac{\pi - 2\beta \exp(-\beta)}{\beta^2 + \frac{\pi^2}{4}} \exp\left(\frac{\pi}{2} \xi\right) \sin\left(\frac{\pi}{2} \xi\right) \frac{\exp(i\omega t) - \exp(-\tau)}{\rho + i\omega} \quad (17)$$

193 where $\rho = D[\pi^2 + \nu^2]/(4L^2)$ and $\tau = \rho t$. The time scale of the hydraulic system, τ_c , is
194 referred to as the hydraulic response time (Gelhar, 1993). Here, it is interpreted as the
195 characteristic time for a change in upstream discharge to reach the downstream end of the
196 stream. For most practical applications, it is much greater than unity, which is the main
197 interest of this study.

198 The use of Eq. (17), in turn, simplifies Eqs. (13) and (16), respectively, to

$$\begin{aligned}
199 \quad \sigma_{\varrho}^2(X, t) &= \frac{D^2}{L^2} \left(\nu + \frac{1}{\mu}\right)^2 \frac{[\pi - 2\beta \exp(-\beta)]^2}{(\beta^2 + \frac{\pi^2}{4})^2} \exp(\nu\xi) \sin^2\left(\frac{\pi}{2} \xi\right) \\
200 \quad &\times \int_{-\infty}^{\infty} \frac{1 - 2\exp(-\tau) \cos(\omega t) + \exp(-2\tau)}{\omega^2 + \rho^2} S_{qq}(\omega) d\omega \quad (18)
\end{aligned}$$

$$\begin{aligned}
201 \quad S_{\omega\omega}(X, t, \omega) &= \frac{D^2}{L^2} \left(\nu + \frac{1}{\mu}\right)^2 \frac{[\pi - 2\beta \exp(-\beta)]^2}{(\beta^2 + \frac{\pi^2}{4})^2} \exp(\nu\xi) \sin^2\left(\frac{\pi}{2}\xi\right) \\
202 \quad &\times \frac{1 - 2\exp(-\tau)\cos(\omega t) + \exp(-2\tau)}{\omega^2 + \rho^2} S_{qq}(\omega) \quad (19)
\end{aligned}$$

203 Equation (19) states that the spectrum of the discharge is a result of a competitive relation
204 between the signal frequency and the properties of the stream channel and inflow.
205 Generally, it is very difficult to quantify the variability of inflow rate. Equation (19) thus
206 provides information about the nature of inflow processes. For example, on the basis of
207 an observed discharge perturbation time series with known hydraulic parameters, the
208 nature of inflow processes may be determined from Eq. (19). After normalizing by the
209 spectral density $S_{qq}(-)$, the evolutionary power spectral density Eq. (19) as a function of
210 dimensionless frequency for various time scales and locations are graphed in Figures 1a-b,
211 respectively. It shows that the spatial variation of spectral amplitude associated with a
212 given frequency increases with the time and the distance from the upstream boundary as
213 well. It reveals that the variability of flow discharge increases with time and distance.

214

215 **4. Closed-form expressions for the variance and spectral density of discharge** 216 **fluctuations**

217

218 In this work, the spectrum of red noise is used to evaluate Eqs. (18) and (19) explicitly.
219 The analysis of discharge variability in this section assumes an exponential form for the
220 autocovariance function of the random fluctuations in the peak inflow rate (Jin and Duffy,
221 1994; Kumar and Duffy, 2009), namely,

222 $C_{qq}(\ell_s) = \sigma_q^2 \exp\left(-\frac{|\ell_s|}{\lambda}\right)$ (20a)

223 which has the following spectral density function

224 $S_{qq}(\omega) = \frac{\sigma_q^2 \lambda}{\pi(1 + \lambda^2 \omega^2)}$ (20b)

225 where ℓ_s is the time lag and σ_q^2 and λ are, respectively, the variance and temporal
226 correlation scale of peak inflow rate fluctuations.

227 Upon substituting Eq. (20b) into Eq. (18) and integrating it over the frequency
228 domain, one obtains the following expression for the variance of flow discharge
229 fluctuations as

230
$$\sigma_Q^2(X, t) = 16 \sigma_q^2 L^2 \frac{(\nu + \frac{1}{\mu})^2}{(\pi^2 + \nu^2)^2} \frac{[\pi - 2\beta \exp(-\beta)]^2}{(\beta^2 + \frac{\pi^2}{4})^2} \exp(\nu\xi) \sin^2\left(\frac{\pi}{2}\xi\right)$$

231
$$\times \tau_R \left\{ \frac{1 + \exp(-2\tau)}{1 + \tau_R} - 2 \frac{\exp(-\tau)}{1 - \tau_R^2} \left[\exp(-\tau) - \tau_R \exp\left(-\frac{\tau}{\tau_R}\right) \right] \right\}$$
 (21)

232 where $\tau_R = \rho\lambda$. Equation (21) indicates a linear relationship between the variances of
233 fluctuations in the flow discharge and inflow rate, implying that the flow variability
234 increases linearly with the heterogeneity of the inflow rate. With Eq. (20b), the resulting
235 expression for the evolutionary power spectral density in Eq. (19) is given by

236
$$S_{QQ}(X, t, \omega) = \frac{\sigma_q^2 D^2}{\pi L^2} \left(\nu + \frac{1}{\mu}\right)^2 \frac{[\pi - 2\beta \exp(-\beta)]^2}{(\beta^2 + \frac{\pi^2}{4})^2} \exp(\nu\xi) \sin^2\left(\frac{\pi}{2}\xi\right)$$

237
$$\times \frac{1 - 2\exp(-\tau)\cos(\omega t) + \exp(-2\tau)}{\omega^2 + \rho^2} \frac{\lambda}{1 + \lambda^2 \omega^2}$$
 (22)

238 Figure 2 shows the plot of the dimensionless variance of discharge fluctuations in Eq.

239 (21) as a function of dimensionless time for various dimensionless temporal correlation
240 scales of inflow rate fluctuations. The figure indicates that the variability of flow
241 discharge induced by the variation of inflow rate increases gradually with time toward its
242 asymptotic value at large time. The correlation scale provides a measure of the strength of
243 the persistence of fluctuations around the mean. It is anticipated that the stochastic
244 processes will exhibit rather clear trends with relatively little noise (a smoother data
245 profile) if the correlation scale is larger. In other words, the temporal fluctuations in
246 inflow rate are either consistently above or below the profile of mean inflow rate in the
247 case of a larger temporal correlation scale. Those larger inclusions in turn lead to larger
248 deviations of flow discharge from the initially uniform steady-state flow discharge.

249 Variation of flow discharge with the distance from the upstream boundary is
250 depicted in Figure 3 according to Eq. (21). As noted in the figure, the variability of flow
251 discharge grows monotonically with distance, implying that due to the naturally inherent
252 variability of lateral inflow, uncertainty in the flow discharge calculations from a
253 deterministic model increases with the distance from the upstream boundary. In other
254 words, the prediction of flow discharge distribution based on the deterministic simulation
255 results is subject to the largest uncertainty in the downstream region. The downstream
256 region is important in most real applications of modeling, and Eq. (21) provides a way of
257 assessing the variation around the deterministic model prediction.

258 Many practical applications involving prediction over a large scale require
259 measurement of uncertainty. Standard deviation is the best way to accomplish that. In this
260 sense, the prediction results from a deterministic model are treated as the mean values.
261 The mean value plus one standard deviation (square root of Eq. (21)) provides a rational

262 basis for extrapolating relatively small-scale field observations to these large space scales.
263 Moreover, the likelihood of the flow discharge falling in the range of one standard
264 deviation greater and smaller than the mean is about 68.27%.

265

266 **5. Conclusions**

267

268 The problem of fluctuations in flow discharge in open channels in response to temporal
269 changes in lateral inflow rate is investigated stochastically for a finite flow domain. In
270 this study, the inflow perturbation field is modeled as a temporally stationary random
271 process. For a complete stochastic description of flow discharge variability, expressions
272 for the covariance function and evolutionary power spectral density of the random flow
273 discharge perturbation process are developed. These expressions are obtained using a
274 spectral representation theory. The variance relation developed here provides a rational
275 basis for quantifying the uncertainty in applying the deterministic model.

276 This work represents an initial step in stochastic study of the effect of temporal
277 variation of lateral inflow on the stream flow discharge variability. To take the advantage
278 of a closed-form solution, the linearized diffusion wave equation (2) is therefore used as
279 the starting point for this research. It is important to recognize that the results developed
280 in this work are valid only for the case of small variations in flow discharge around an
281 initially uniform flow regime.

282 It is found from our closed-form expressions that the discharge variability in stream
283 channels induced by the temporal changes in lateral inflow rate increases gradually with
284 time toward its asymptotic value at large time. A larger temporal correlation scale of

285 inflow rate fluctuations which is of a more persistence of inflow perturbation process will
286 introduce more variability of the flow discharge. The increase of discharge variability
287 with the distance from the upstream boundary suggests that prediction of flow discharge
288 distribution in channels using a deterministic model is subject to large uncertainty at the
289 downstream reach of the stream.

290

291 **Acknowledgements.** This research work is supported by the Taiwan Ministry of Science
292 Technology under the grants NSC 101-2221-E-009-105-MY2,
293 102-2221-E-009-072-MY2 and NSC 102-2218-E-009-013-MY3. We are grateful to the
294 Editor Prof. Zhongbo Yu and anonymous referees for constructive comments that
295 improved the quality of the work.

296

297 **References**

298 Bewket, W., and Lal, R.: Recent spatiotemporal temperature and rainfall variability and
299 trends over the Upper Blue Nile River Basin, Ethiopia, *Int. J. Climatol.*, 34(7),
300 2278-2292, 2014.

301 Capsoni, C., Fedi, F., Magistroni, C., Paraboni, A., and Pawlina, A.: Data and theory for a
302 new model of the horizontal structure of rain cells for propagation applications,
303 *Radio Sci.*, 22(3), 395-404, 1987.

304 Daluz Viera, J. H.: Conditions governing the use of approximations for the Saint-Venant
305 equations for shallow water flow, *J. Hydrol.*, 60, 43-58, 1983.

306 De Michele, C., Bernardara, P.: Spectral analysis and modeling of space-time rainfall

307 fields. Atmos. Res., 77(1-4), 124-136, 2005

308 Dooge, J. C. I. and Harley, B. M.: Linear routing in uniform channels, Proc. Int. Hydrol.
309 Symp., 1, 57-63, 1967.

310 Dooge, J. C. and Napiorkowski, J. J.: The effect of the downstream boundary condition in
311 the linearized St. Venant equations, Quarterly J. Mech. Appl. Math., 40, 245-256,
312 1987.

313 Duan, Q., Sorooshian, S., and Gupta, V.: Effective and efficient global optimization for
314 conceptual rainfall-runoff models, Water Resour. Res., 28(4), 1015-1031, 1992.

315 Féral, L., Sauvageot, H., Castanet, L., and Lemorton, J.: A new hybrid model of the rain
316 horizontal distribution for propagation studies: 1. Modeling of the rain cell, Radio
317 Sci., 38(3), 1056, doi:10.1029/2002RS002802, 2003.

318 Fournier, B., Guenat, C., Bullinger-Weber, G., and Mitchell, E. A. D.: Spatio-temporal
319 heterogeneity of riparian soil morphology in a restored floodplain, Hydrol. Earth
320 Syst. Sci., 17(10), 4031-4042, 2013.

321 Gelhar, L. W.: *Stochastic Subsurface Hydrology*, Englewood Cliffs, New Jersey, Prentice
322 Hall, 1993.

323 Goodrich, D. C., Lane, L. J., Shillito, R. M., Miller, S. N., Syed, K. H., and Woolhiser, D.
324 A.: Linearity of basin response as a function of scale in a semiarid watershed,
325 Water Resour. Res., 33(12), 2951-2965, 1997.

326 Govindaraju, R. S.: Modeling overland flow contamination by chemicals mixed in
327 shallow soil horizons under variable source area hydrology, Water Resour. Res.,
328 32(3), 753-758, 1996.

329 Haberlandt, U., Ebner von Eschenbach, A.-D., and Buchwald, I.: A space-time hybrid
330 hourly rainfall model for derived flood frequency analysis, *Hydrol. Earth Syst. Sci.*,
331 12(6), 1353-1367, 2008.

332 Henderson, F. M.: Flood waves in prismatic channels, *ASCE J. Hydr. Div.*, 89(HY4),
333 39-67, 1963.

334 Jencso, K. G., McGlynn, B. L., Gooseff, M. N., Wondzell, S. M., Bencala, K. E., and
335 Marshall, L. A.: Hydrologic connectivity between landscapes and streams:
336 Transferring reach- and plot-scale understanding to the catchment scale, *Water*
337 *Resour. Res.*, 45, W04428, doi:10.1029/2008WR007225, 2009.

338 Jin, M. and Duffy, C.J.: Spectral and bispectral analysis for single and multiple input
339 nonlinear phreatic aquifer systems, *Water Resour. Res.*, 30 (7), 2073-2095, 1994.

340 Kazezyılmaz-Alhan, C. M.: An improved solution for diffusion waves to overland flow,
341 *Applied Mathematical Modelling*, 36(9), 4165-4172, 2012.

342 Khasraghi, M. M., Sefidkouhi M. A. G., and Valipour M.: Simulation of open- and
343 closed-end border irrigation systems using SIRMOD, *Arch. Agron. Soil Sci.*, 61(7),
344 929-941, 2015.

345 Kumar, M. and Duffy, C.J.: Detecting hydroclimatic change using spatio-temporal
346 analysis of time series in Colorado River Basin, *J Hydrol.*, 374(1-2), 1-15, 2009.

347 Lane, L. J.: Distributed model for small semiarid watersheds, *Hydraul. Div. Am. Soc.*
348 *Civ. Eng.*, 108(HY10), 1114-1131, 1982.

349 Li, S.-G. and McLaughlin, D.: A nonstationary spectral method for solving stochastic
350 groundwater problems: Unconditional analysis, *Water Resour. Res.*, 27(7),
351 1589-1605, 1991.

352 Moramarco, T., and Singh, V. P.: Accuracy of kinematic wave and diffusion wave for
353 spatial-varying rainfall excess over a plane, *Hydrol. Process.*, 16(17), 3419-3435,
354 2002.

355 Morris, E. M.: The effect of small slope approximation and lower boundary conditions on
356 solution of Saint Venant equations, *J Hydrol.*, 40, 31-47, 1979.

357 Moussa, R.: Analytical Hayami solution for the diffusive wave flood routing problem
358 with lateral inflow. *Hydrol. Process.*, 10(9), 1209-1227, 1996.

359 Ogden, F. L. and Julien, P. Y.: Runoff sensitivity to temporal and spatial rainfall
360 variability at runoff plane and small basin scales, *Water Resour. Res.*, 29(8),
361 2589-2597, 1993.

362 Ponce, V. M., Li, R. M., and Simons, D. B.: Applicability of kinematic and diffusion
363 models, *Journal of the Hydraulics Division, ASCE*, 104(HY3), 353-360, 1978.

364 Ponce, V. M.: Generalized diffusion wave equation with inertial effects, *Water Resour.*
365 *Res.*, 26 (5), 1099-1101, 1990

366 Priestley, M. B.: Evolutionary spectra and non-stationary processes. *J. R. Stat. Soc. Ser. B.*,
367 27, 204-237, 1965.

368 Redano, A. and Lorente, J.: Modelling the spatial and temporal distribution of rainfall
369 intensity at local scale, *Theor. Appl. Climatol.* 47, 25-32, 1993.

370 Riley, W. J. and Shen, C.: Characterizing coarse-resolution watershed soil moisture
371 heterogeneity using fine-scale simulations, *Earth Syst. Sci.*, 18(7), 2463-2483,
372 2014.

373 Ruiz-Villanueva, V., Borga, M., Zoccatelli, D., Marchi, L., Gaume, E., and Ehret, U.:
374 Extreme flood response to short-duration convective rainfall in South-West
375 Germany, *Hydrol. Earth Syst. Sci.*, 16(5), 1543-1559, 2012.

376 Schumann, G., Lunt, D. J., Valdes, P. J., de Jeu, R. A. M., Scipal, K., and Bates, P. D.:
377 Assessment of soil moisture fields from imperfect climate models with uncertain
378 satellite observations, *Earth Syst. Sci.*, 13(9), 1545-1553, 2009

379 Singh, V. P., and Aravamuthan V.: Accuracy of kinematic wave and diffusion wave
380 approximations for time-independent flows, *Hydrol. Process.*, 9(7), 755-782, 1995.

381 Sivakumar, B., Berndtsson, R., Olsson, J., Jinno, K., and Kawamura, A.: Dynamics of
382 monthly rainfall-runoff process at the Gota basin: A search for chaos, *Hydrol. Earth
383 Syst. Sci.*, 4(3), 407-417, 2000.

384 Sivapalan, M., Bates, B. C., and Larsen, J. E.: A generalized, non-linear, diffusion wave
385 equation: theoretical development and application, *J Hydrol.*, 192, 1-16, 1997.

386 Tsai, C. W.-S., Yen B. C.: Linear analysis of shallow water wave propagation in open
387 channels, *J. Eng. Mech.*, 127, 459-472, 2001.

388 Valipour, M.: Critical areas of Iran for agriculture water management according to the
389 annual rainfall, *Eur. J. Sci. Res.*, 84(4), 600-608, 2012.

390 Valipour, M.: Long-term runoff study using SARIMA and ARIMA models in the United
391 States, *Meteorol. Appl.*, doi: 10.1002/met.1491, early view, 2015.

392 Wheeler, H. S., Isham, V. S., Cox, D. R., Chandler, R. E., Kakou, A., Northrop, P. J., Oh,
393 L., Onof, C., and Rodriguez-Iturbe I.: Spatial-temporal rainfall fields: modelling
394 and statistical aspects, *Hydrol. Earth Syst. Sci.*, 4(4), 581-601, 2000.

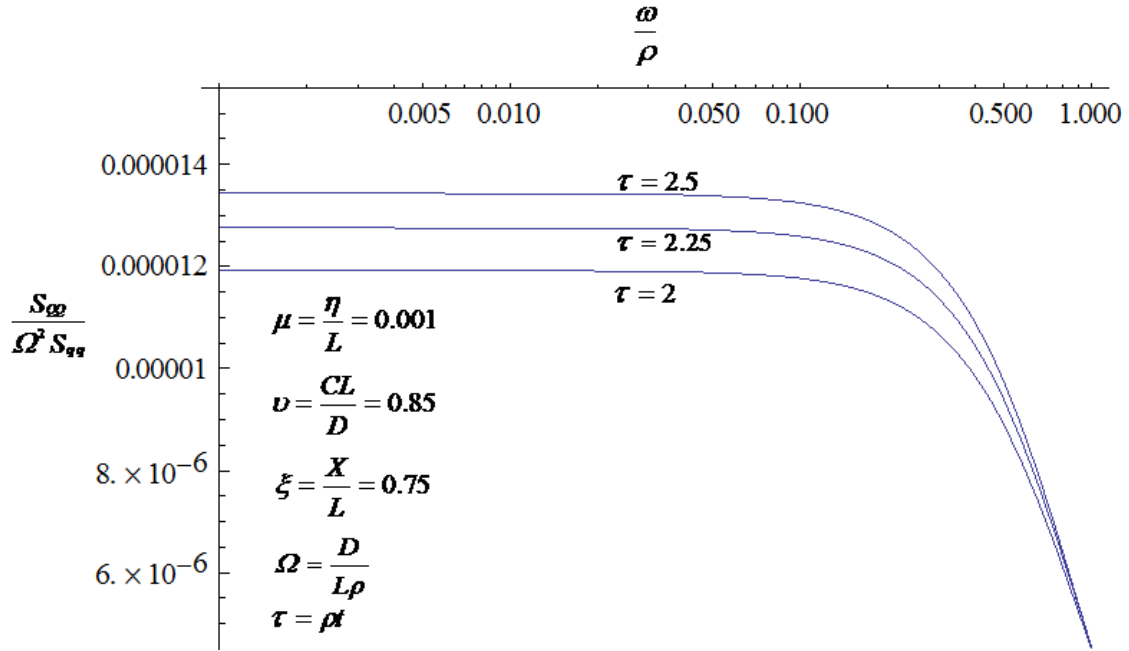
395 Yen, B. C. and Tsai, C. W.-S.: On noninertia wave versus diffusion wave in flood routing,
396 J Hydrol., 244(1-2), 97-104, 2001.

397 Zhang, X., Hogg, W. D., and Mekis, E.: Spatial and temporal characteristics of heavy
398 precipitation events over Canada, J. Climate, 14(9), 1923-1936, 2001.

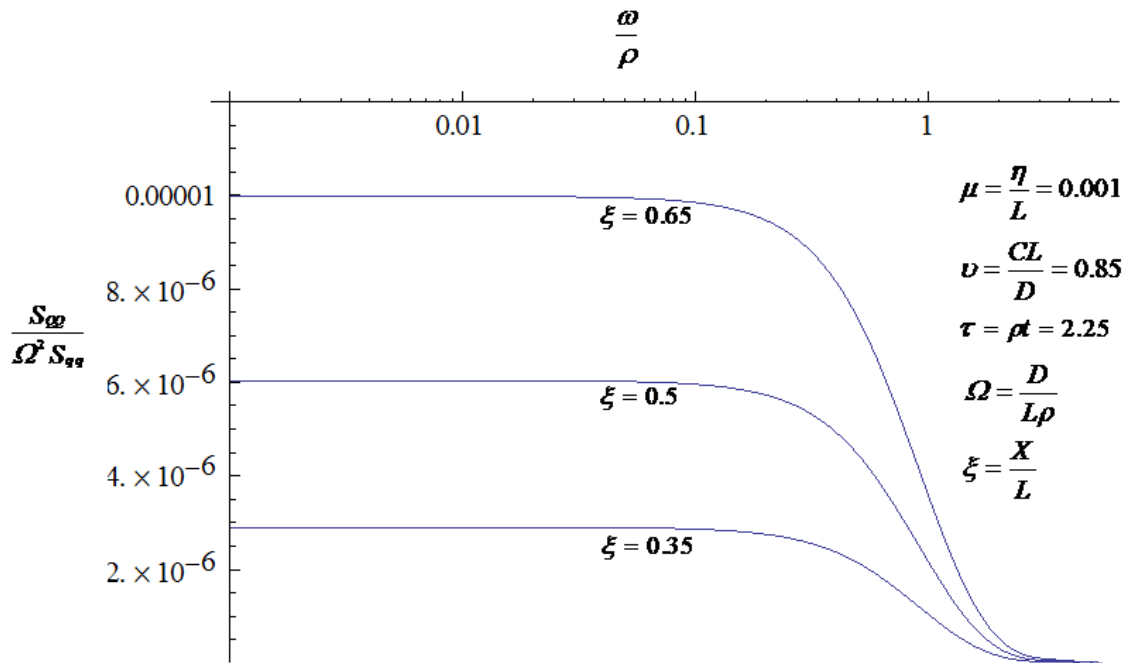
399

400 **Figures**

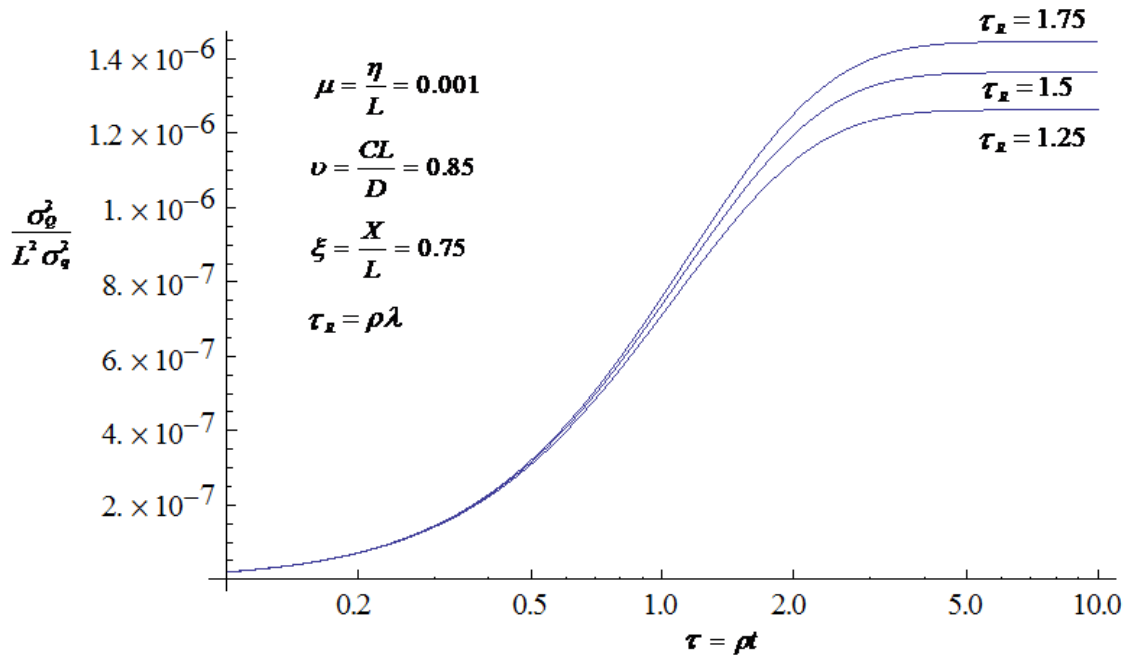
401 a)



403 b)

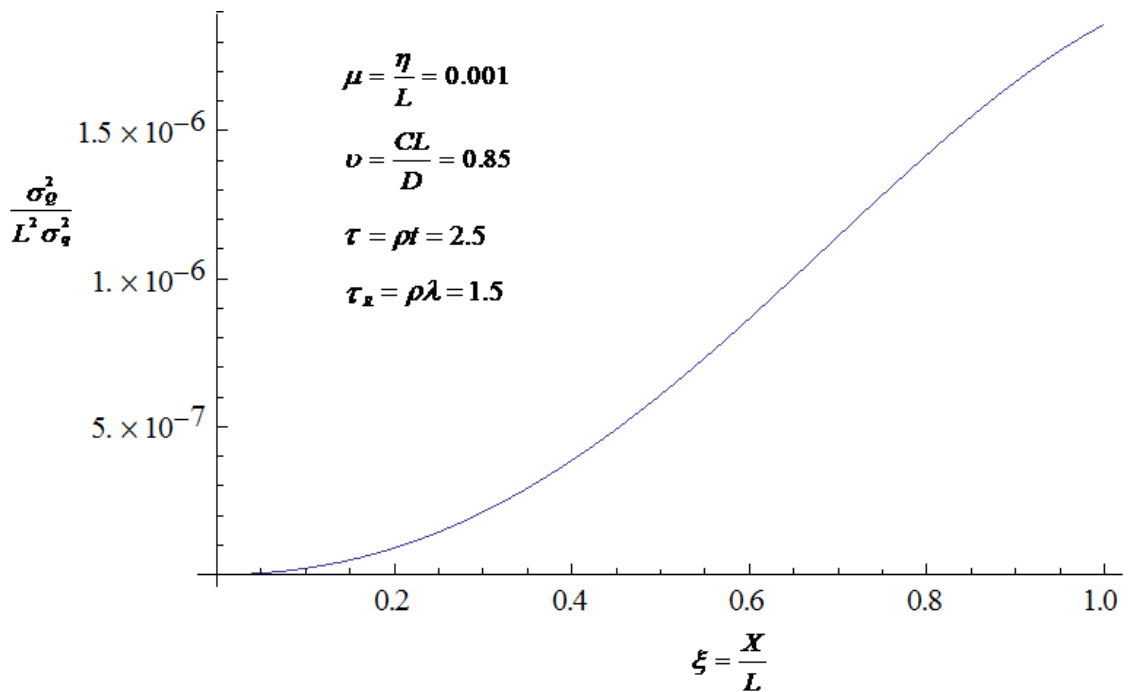


405 **Fig. 1.** Dimensionless evolutionary power spectral density as a function of dimensionless
 406 frequency for various (a) time scales and (b) locations.



407

408 **Fig.2.** Dimensionless variance of discharge fluctuations as a function of dimensionless
 409 time for various dimensionless temporal correlation scales of inflow rate
 410 fluctuations.



411

412 **Fig. 3.** Dimensionless variance of discharge fluctuations as a function of dimensionless
 413 distance from the upstream boundary.